P1.16 ADIABATIC LAPSE RATES IN TORNADIC ENVIRONMENTS

Matthew D. Parker*
Convective Storms Group, The Mesoscale Nexus in Atmospheric Sciences
North Carolina State University, Raleigh, North Carolina

1. INTRODUCTION

A brief survey reveals numerous examples of tornadoes that have occurred in environments with adiabatic, or nearly-adiabatic, lapse rates. One reasonable hypothesis for this relationship posits that steeper temperature lapse rates entail more environmental CAPE. This in turn would engender greater updraft buoyancy, a larger vertical gradient in updraft buoyancy above cloudbase, and therefore more rapid generation and stretching of vertical vorticity within the strengthened updraft. These physical linkages seem relatively staightforward.

However, another notable property of adiabatic environments is that they prohibit gravity wave propagation. In this case, a storm's induced environmental subsidence does not engender the temperature perturbations needed to move the waves. In stabler environments, gravity waves quickly disperse convective heating to the far field through propagation. In the absence of such gravity waves, slower advective mechanisms are needed to disperse the convective heating. Because these mechanisms are less efficacious, a great deal of the convective latent heating remains trapped in the convective column for comparatively long periods of time. This study is a preliminary attempt to assess the possible roles of gravity waves in tornadic vs. non–tornadic environments.

2. METHOD

A straightforward approach to this problem might be simply to change the lapse rate within a moist simulation of a supercell or other possibly tornadic convective storm. Changes to the thermodynamic sounding in a full–physics convection simulation would entail changes in CAPE, which in turn would lead to a storm that is stronger. Although this is almost certainly a consideration in the tornado problem, in this case we seek specifically to address the role of gravity waves in dissipating heating from a storm within a variety of environments. Accordingly, we use a more idealized method.

* *Corresponding author address:* Matthew D. Parker, Department of Marine, Earth, & Atmospheric Sciences, North Carolina State University, Campus Box 8208, Raleigh, NC 27695–8208. E-mail: mdparker@ncsu.edu

This preprint describes preliminary results from the Advanced Regional Prediction System (ARPS), version 5.1.0. The model was configured to be run in 2D, with only dry dynamics. The model had both horizontal and vertical grid spacings of 100 m, with a domain width of 100 km and a domain depth of 15 km. The environments for the simulations included an idealized stratosphere above 10 km AGL, which had a constant lapse rate of $d\theta/dz = $0.016 K/m. The three simulations summarized here had varied tropospheric (0-10 km AGL) lapse rates. In the first, the 0-10 km lapse rate was set to a modest value of $d\theta/dz = $0.004 K/m; this is the "control" simulation. In the second, the 0-10 km lapse rate was set to the dry adiabatic value ($d\theta/dz = $0 K/m); this is the "adiabatic" simulation. Finally, in the third simulation, the 0-3 km lapse rate was set to the dry adiabatic value ($d\theta/dz = $0 K/m), and the 3-10 km lapse rate was set to the control lapse rate ($d\theta/dz = $0.004 K/m); this is the "shallow adiabatic" simulation, which might mimic a deep well-mixed boundary layer and/or the presence of an elevated continental mixed-layer such as might be advected over the Plains from the higher terrain to the south or west.

The present results represent a first cut at the problem, using an admittedly limited model configuration. Additional, more realistically-configured 3D simulations are currently ongoing using the Advanced Research core of the Weather Research and Forecasting (WRF) model, version 2.1.

In order to achieve the goal of mimicking an unvarying base storm withing this variety of environments (and because the simulations included no water substance), a fixed region of latent heating was included in the simulations. This artificial heating had a horizontal footprint and vertical profile consistent with the main updraft of a supercell produced by a full-physics simulation with the same numerical model (contact the author for more details). Even though, in nature, latent heating rates and updraft buoyancy undoubtedly vary with the environmental lapse rates, in this experiment the simulated differences in the evolution of the wind and pressure fields are attributable not to the storm, but to the *environment's response to the storm*.

3. RESULTS

In the control environment, gravity waves are very effective in propagating heating away from the column where it is introduced. After 8 minutes of simulated heating, the predominant temperature signature is one of an outward–propagating wave of warming through subsidence (Fig. 1a); the air in the heated column is scarcely warmer than the base state. The pressure field associated with the simulated convective heating produces a downward–directed perturbation pressure gradient force in the near environment. In response, environmental air begins to sink, becomes warmer than its surroundings, and a propagating gravity wave commences. Within the first 4 minutes of the control simulation, the surface pressure falls to a deficit of 0.83 hPa, after which it begins to slowly recover as the warm anomaly is propagated away (Fig. 1a).

In contrast, in the adiabatic simulation gravity waves are prohibited. Much as in the control environment, a perturbed pressure field develops which entails downward accelerations in the nearby environment. However, in the adiabatic case, this subsidence does not entail temperature perturbations. As a result, the local warming cannot be propagated away to the far field. Instead, heating accumulates in the vertical column where it has been introduced (Fig. 1c). Therefore, the adiabatic case experiences continuing pressure falls through the first 8 minutes of simulation (and beyond), at which time the surface pressure deficit beneath the heated column is 1.97 hPa (Fig. 1c).

In response to these perturbed pressure fields, radial convergence develops beneath the heated column (Figs. 1d, 2). In a background state with pre–existing vertical vorticity (which the present idealized simulations *do not* possess), such convergence entails increasing vertical vorticity. During the 20 simulated minutes, the convergence of vorticity alone would increase the base state vorticity by 1241% in the adiabatic simulation, versus only 22% in the control simulation. In other words, in the adiabatic environment, the convergence term may increase the vertical vorticity by more than an order of magnitude over the control environment.

The horizontal and vertical advection terms would partly offset such a large local increase in vorticity through convergence. However, it is also worth nothing that the present, simple simulations do not permit any feedbacks between the rate of lower tropospheric convergence and the heating. As well, other sources of vorticity such as the tilting of horizontal vorticity into the vertical are unable to be realized in the present idealized configuration. Finally, the present simulations contain no chilling in the proximity of the updraft, which would lead to larger quasi-static radial pressure gradients than the column of heating alone.

Despite these simplifications, the present study sought to isolate the possible impact of the presence or absence of gravity waves, and suggests that this effect can make a difference of one order of magnitude upon one of the terms in the vorticity equation. The cyclostrophic wind fields at t=8 min are consistent with this, showing a deep and intense tangential flow at small radius in the adiabatic case (Fig. 1d), versus a broad and weak tangential flow in the control case (Fig. 1b). Notably, because the heating is trapped locally, in the adiabatic simulations the horizontal scale of the response to the heating closely mirrors the horizontal scale of the artificial heating source (Fig. 1c,d). Narrower, more concentrated heat sources produce even more dramatic results.

The above discussion argues that, no matter how vertical vorticity comes to exist at the surface, the low–level convergence in the adiabatic case should be most effective in concentrating it. Beyond this, however, many current hypotheses for supercellular tornadogenesis focus on the role of the rear flank downdraft in transporting air with large angular momentum to the surface. Apparently, this mechanism most strongly favors tornadogenesis when the downdraft is comparatively warm. Such relatively warm downdrafts would be most likely in situations where chilling from phase changes of water are not required to produce downward accelerations. It is therefore noteworthy that, in the adiabatic case, environmental subsidence does not occur *throughout* the far field because it is not spread over a full spectrum of propagating gravity waves. Instead, it occurs only locally where it is directly forced by the downward–directed perturbation pressure gradient at the edge of the updraft. This downward forcing persists for a sufficiently long time that a dry downdraft in excess of 10 m/s develops in the adiabatic case (Fig. 1d). Without including any of the complex interactions that occur in real supercells, this highly idealized configuration produces an intense updraft–flanking downdraft that arrives at the surface without any negative bouyancy.

In the adabatic simulation, convergence beneath the heat source continues to intensify until roughly t=12 min, after which it decreases (Fig. 2). This is because the surface pressure will not fall indefinitely, even in the adiabatic environment. A cross–section at this time reveals that the warm anomaly, although not propagated away through gravity waves, is at last being advected away from the column in the upper troposphere by the divergent horizontal flow field that has developed (Fig. 3). The key to the differences between the control and adiabatic simulations is that this happens very slowly. In the adiabatic simulation, the warm anomaly can only be moved away at the speed of the horizontal flow that has been produced by the horizontal pressure gradient force:

it takes time for these velocities to become large enough to be effective. In contrast, even the very small wind perturbations that develop early in the control case are enough to propagate the heating away quickly at the intrinsic gravity wave phase speed.

In most regards, the shallow adiabatic case represents a midpoint between the control and adiabatic simulations, bearing some similarities to each (Figs. 1e,f; 2). Heating accumulates in the vertical column, especially within the adiabatic layer, but its integrated effect is less because gravity waves do propagate away heating within the stabler layers aloft. Whereas the fully adiabatic experiment shows the possible extent to which a lack of gravity wave propagation can impact the local fields, other mechanisms are likely important in supplementing this effect in the real world. Even so, the shallow adiabatic simulation resembles the fully adiabatic simulation below 3 km AGL, exhibiting minimized surface pressure and tangential cyclostrophic flow on the horizontal scale of the heating, along with enhanced local subsidence near the updraft edge. This seems to be consistent with the fact that real world environmental lapse rates during tornadogenesis are often nearly adiabatic throughout the lower tropospheric "action area".

4. CONCLUSIONS

Idealized preliminary simulations do indeed reveal that, in environments with adiabatic or nearly adiabatic lapse rates, latent heating in convection collects in the vertical column. In short order, this can lead to very large quasi-static pressure falls below cloud base, which in turn imply large values of radial inflow (convergence of vertical vorticity) and a significant cyclostrophic flow field. In tandem with this, environmental subsidence is initially constrained to be very near the storm updraft, which could potentially play a role in the initiation of an RFD without the need for precipitation loading or chilling from phase changes.

The working hypothesis is that sub-cloud vortices in adiabatic and nearly-adiabatic environments intensify rapidly because gravity waves are inhibited; this process may act independently or augment other recently-proposed tornadogenesis mechanisms. This hypothesis is attractive because it suggests a reason for tornadoes' existence: tornadoes play a key role in entropy redistribution when storms cannot stabilize their environments through gravity waves.

5. FUTURE STUDIES

More sophisticated numerical experiments are ongoing. But, in order to fully address this and other hypothesized tornado mechanisms, the thermodynamic environment of both tornadic and non-tornadic supercells needs to be characterized with fine temporal and reasonable spatial resolution. The author eagerly anticipates such measurements in the coming years. Such studies may resolve a gap in our knowledge base and advance the science of tornado forecasting.

ACKNOWLEDGMENTS

This line of research originated and evolved through fruitful discussions with P. Haertel and J. Nachamkin. The simulations shown in this preprint were made with the Advanced Regional Prediction System (ARPS), which was developed by the Center for Analysis and Prediction of Storms (CAPS), University of Oklahoma. The ongoing simulations are being performed using the High Performance Computing center at NCSU, whose staff–members have been of great assistance.

REFERENCES

Supplemental references available: please contact the author.

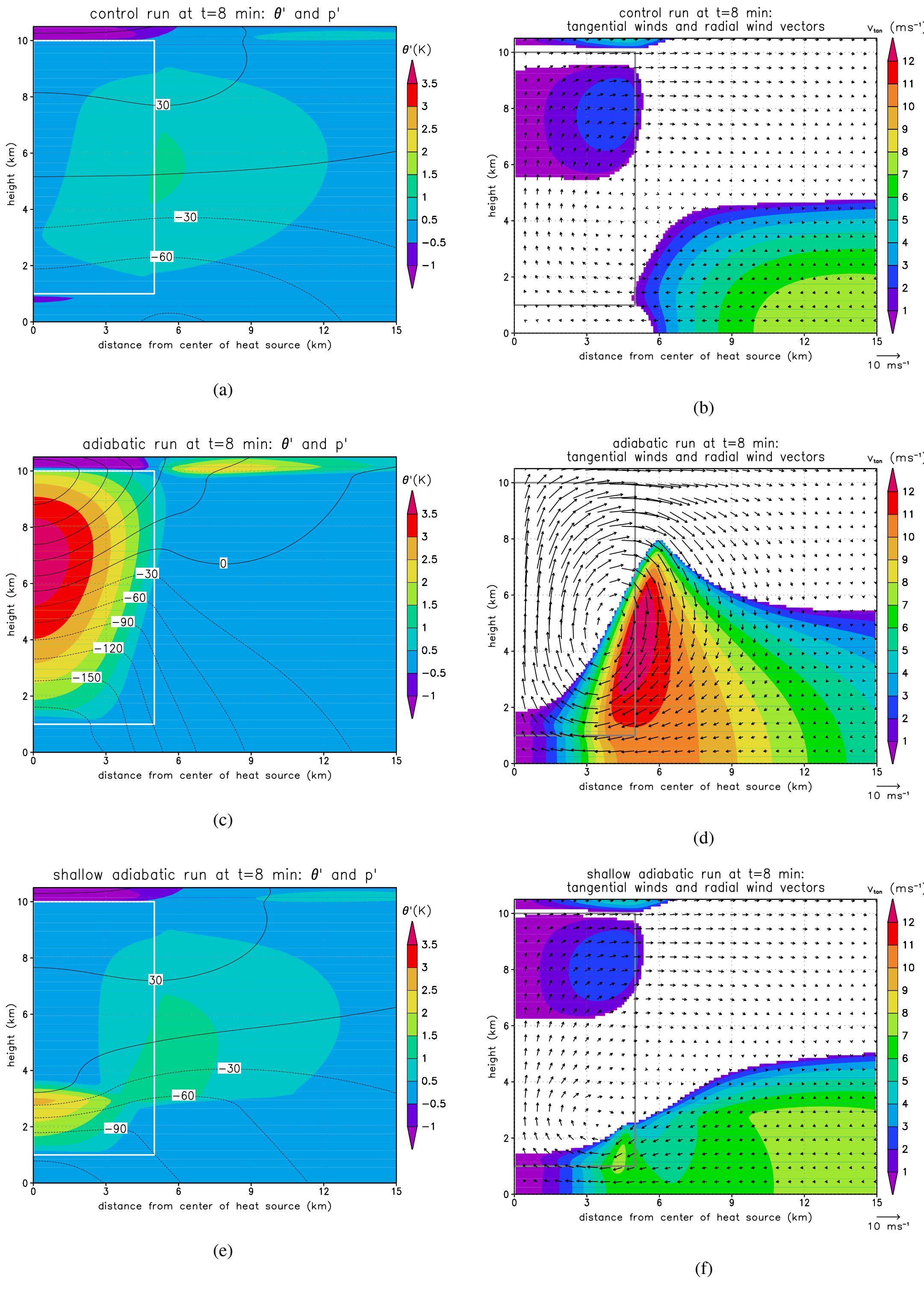

Figure 1: Vertical cross–sections after 8 minutes. Panels a,c,e: potential temperature perturbation (K, shaded) and pressure perturbation (Pa, contoured). Panels b,d,f: cyclostrophic tangential wind (m/s, shaded) and radial flow vectors (m/s, scaled as shown). Panels a,b: for the control (stable) simulation. Panels c,d: for the adiabatic simulation. Panels e,f: for the shallow adiabatic (layers) simulation. The region in which the heating function was applied is outlined in white (a,c,e) or gray (b,d,f).

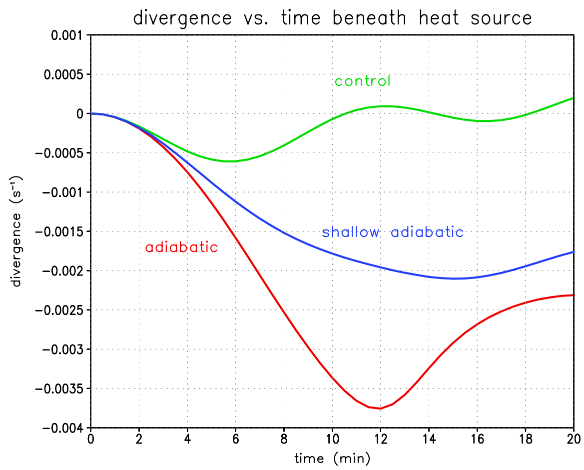

Figure 2: Temporal evolution of the horizontal divergence beneath the applied heat source for the adiabatic (red), control/stable (green), and shallow adiabatic layer (blue) simulations.

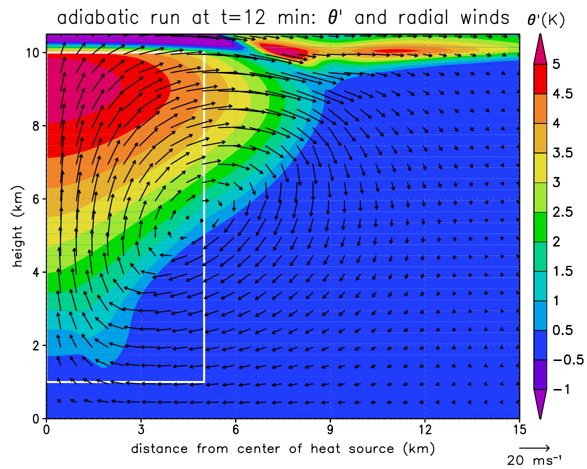

Figure 3: Vertical cross–section of potential temperature perturbation (K, shaded) and radial wind vectors (m/s, scaled as shown) for the adiabatic simulation after 12 minutes. The region in which the heating function was applied is outlined in white. Note that the shading and vectors are scaled differently than in Fig. 1.